

X-Ray Optics

Introduction

1. X-ray Reflection

- Total External Reflection
- Fresnel's Equations

2. Ideal Mirrors

- Figure
- Scattering

3. Practical Mirrors

- Configurations
- Manufacture
- Requirements

Why do we Use X-Ray Optics?

Introduction:

1. To achieve the best, 2-dimensional angular resolution
 - Distinguish nearby sources, different regions of the same source
 - Use morphology to apply models or intuition into the physical processes
 - Freedom from the universally incorrect hypothesis of spherical symmetry
2. As a collector to “gather” weak fluxes of photons
3. As a concentrator, so that the image photons interact in such a small region of the detector that background is negligible or small
4. To serve with high spectral resolution dispersive spectrometers such as transmission or reflection gratings.
5. To simultaneously measure both the sources of interest, and the contaminating background using other regions of the detector.

X-Ray Reflection: Zero Order Principles:

Gursky, H., and Schwartz, D. 1974, in "X-Ray Astronomy," R. Giacconi and H. Gursky eds., (Boston: D. Reidel) Chapter 2, pp 71-81; Aschenbäch, B. 1985, Rep. Prog. Phys. 48, 579.

X-rays undergo total external reflection at small grazing angles. An analogy is skipping stones on water. Scattering of any wave by an ensemble of electrons is coherent only in very special directions; namely, the familiar

Angle of Incidence equals Angle of Reflection, $\phi_i = \phi_o$.

We also have Snell's law,

$$\sin \phi_r = \sin \phi_i / n$$

Where ϕ is the standard angle of incidence from the surface normal, and the complex index of refraction is

$$n = 1 - \delta + i\beta.$$

We have used the subscripts i for the incident photon, o for the reflected or outgoing photon, and r for the refracted photon.

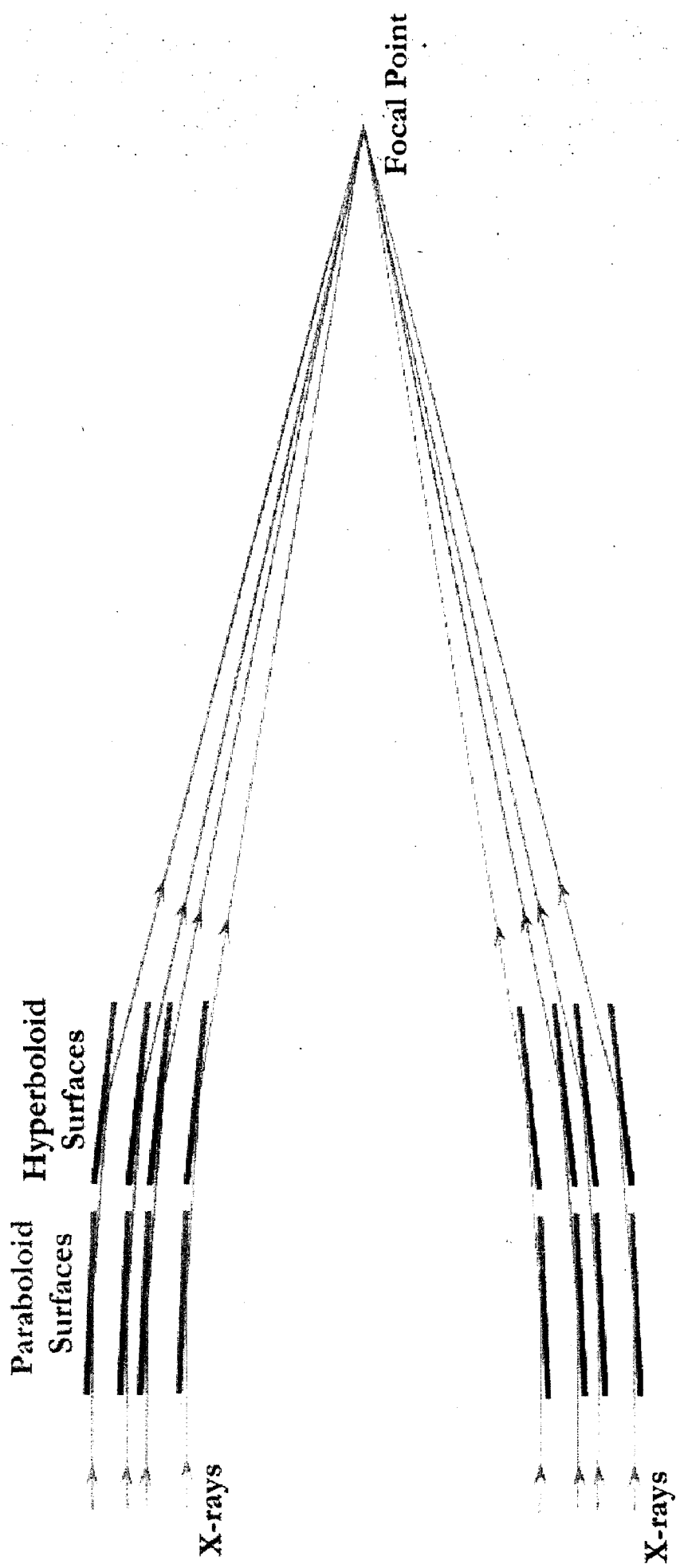
We also note (to be shown later) that $0 < \delta \ll 1$ and $0 < \beta \ll 1$.

To zero-th order, total external reflection works under conditions for which $\sin \phi_r > 1$. Using θ for the "grazing angle," i.e. the angle from a line in the surface to the photon, $\theta = \pi/2 - \phi$, at the limiting condition $\cos \theta_c = n$. For small θ (and forgetting β for the moment)

$$1 - \theta_c^2/2 = 1 - \delta, \text{ and the critical angle is } \theta_c = \sqrt{(2\delta)}.$$

Away from absorption edges, $\delta = r_0 \lambda^2 N_e / (2\pi)$

1. The critical angle decreases inversely proportional to the energy
2. Higher Z materials reflect up to higher energies, at a fixed grazing angle.



Paraboloid
Surfaces

Hyperboloid
Surfaces

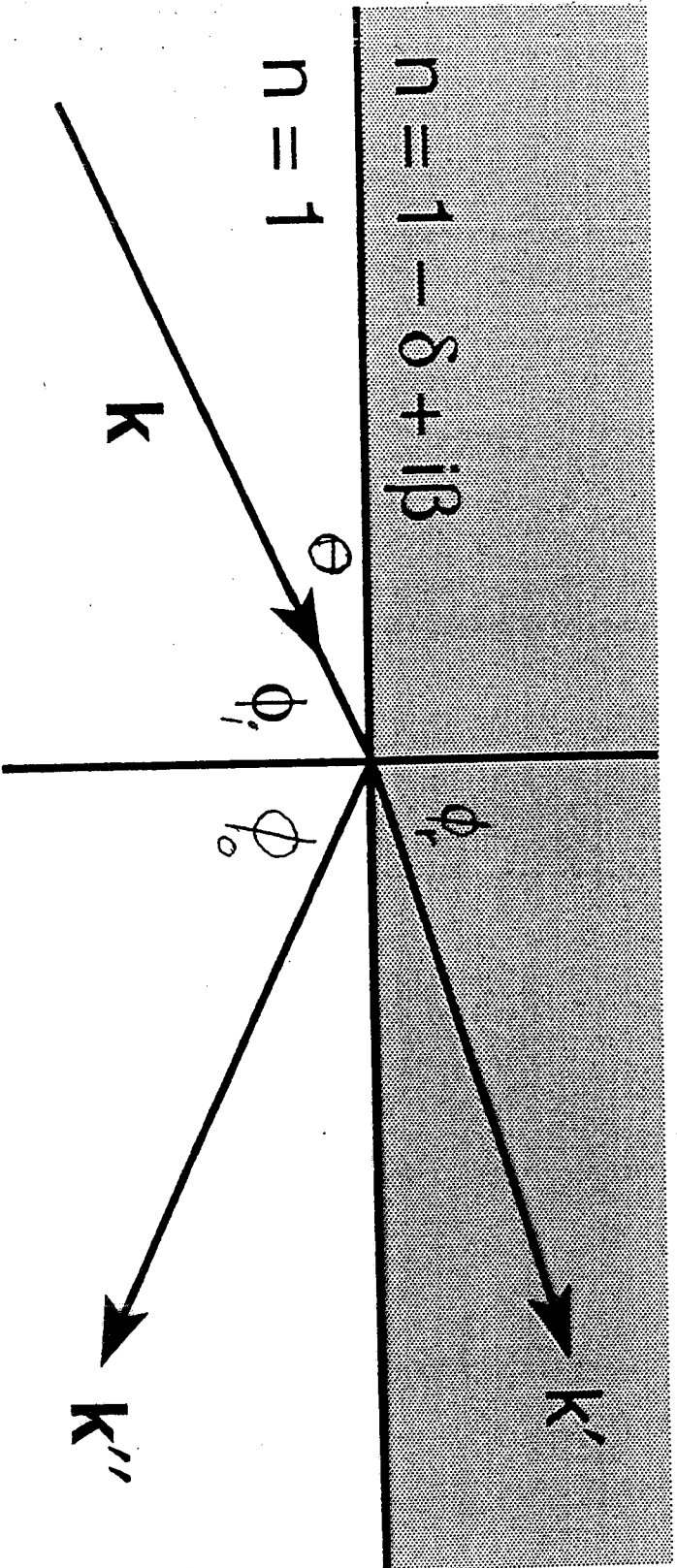
X-rays

X-rays

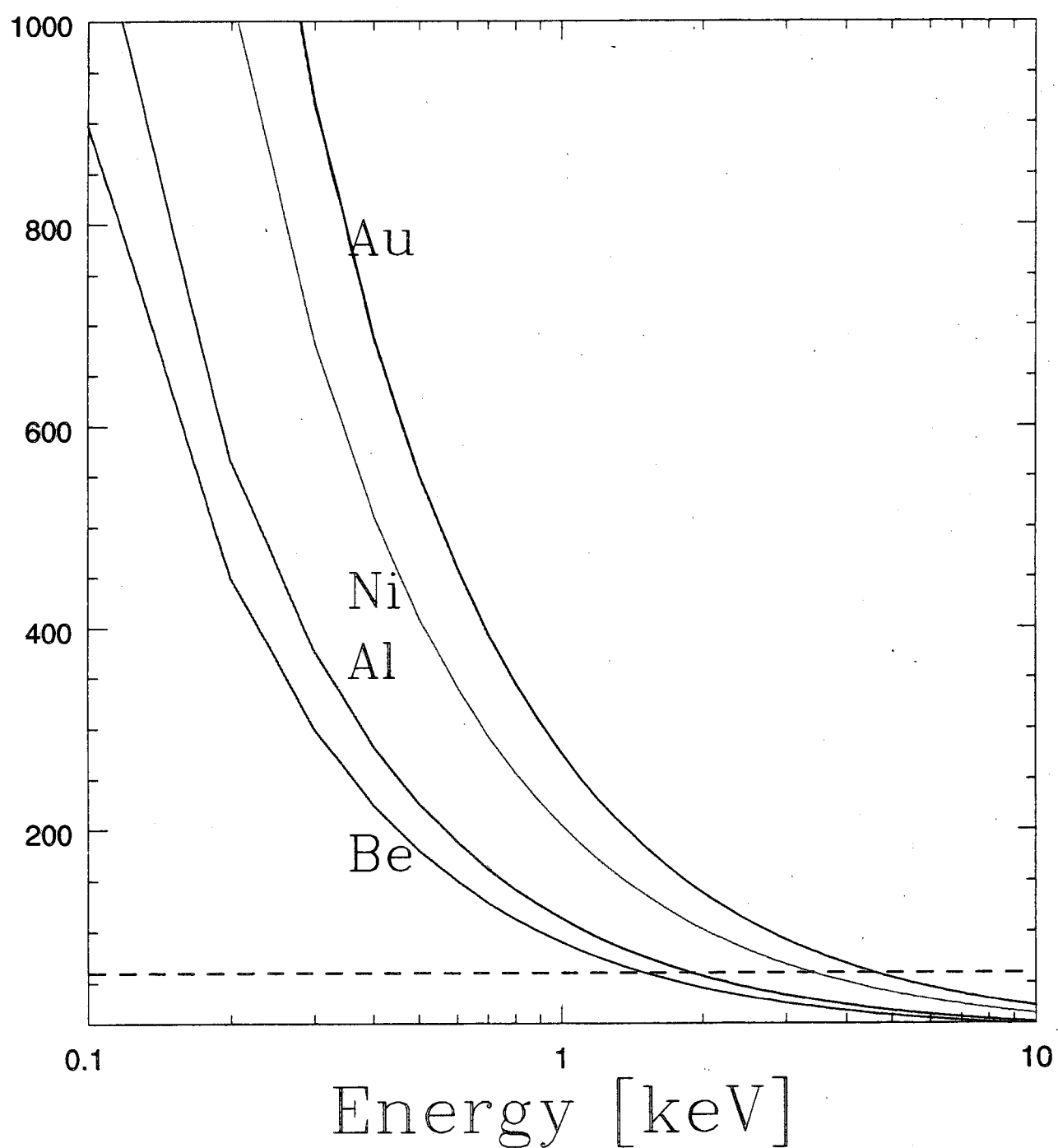
Focal Point



WAVE PROPAGATION AND REFRACTIVE INDEX AT EUV AND SOFT X-RAY WAVELENGTHS



Critical Grazing Angle [arcmin]



SPECIAL TOPIC: Index of Refraction

Attwood, D. 1999, "Soft X-rays and Extreme Ultraviolet Radiation: Principles and Applications, (<http://www.coe.berkeley.edu/AST/sxreuv>)

At the high frequency of X-radiation, the index of refraction can be written in terms of the complex atomic scattering factor $f=(f_1-i f_2)$:

$$n=1-\delta+i\beta = 1-(\rho_a r_0 \lambda^2)/(2 \pi)(f_1-i f_2),$$

where ρ_a is the number density of atoms and r_0 the classical electron radius.

The factor f is a sum over all the electrons, weighted inversely by the difference of the squares of the frequency of the photon and the resonant frequency of the electron and considering a damping factor. However, it can be related directly to a macroscopic observable: the atomic photon absorption cross section μ_a :

$$f_2(E)=(E \mu_a(E))/(2\pi r_0 hc),$$

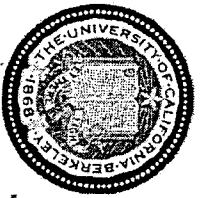
and $f_1=Z +1/(\pi r_0 hc) \int_0^\infty (x^2 \mu_a(E))/(E^2-x^2) dx +\Delta f_{rel}$

So we can readily identify the complex part β , with absorption in the reflecting medium.

If we consider a plane wave, $\mathbf{E}(\mathbf{r},t)=\mathbf{E}_0 e^{-i(\omega t-\mathbf{k}\cdot\mathbf{r})}$, the dispersion relation $\omega/k = c$ in vacuum, and $=c/n$ in a medium with index of refraction n . Substituting $k = (\omega/c) n$ in the reflecting medium, in the direction of propagation we have

$$\mathbf{E}(\mathbf{r},t)=\mathbf{E}_0 e^{-i[\omega t-(\omega/c)(1-\delta+i\beta)r]} = \mathbf{E}_0 e^{-i\omega(t-r/c)} e^{-i(2\pi\delta/\lambda)r} e^{-(2\pi\beta/\lambda)r}.$$

The roles are now clear: we have the wave which would propagate in vacuum, a phase shift caused by the small real deviation from unity, and an *attenuation* caused by the imaginary part of the index of refraction.



Refractive Index from the IR to X-Ray Spectral Region

$$n(\omega) = 1 - \delta + i\beta$$

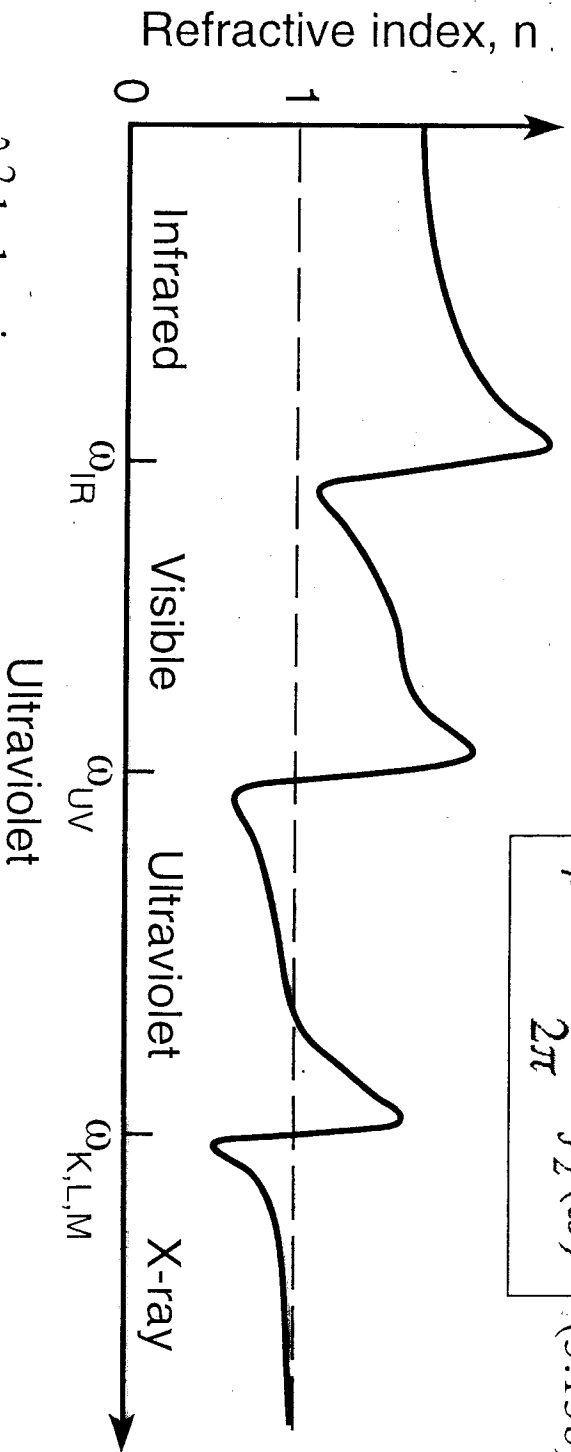
(3.12)

$$\delta = \frac{n_a r_e \lambda^2}{2\pi} f_1^0(\omega)$$

(3.13a)

$$\beta = \frac{n_a r_e \lambda^2}{2\pi} f_2^0(\omega)$$

(3.13b)



- λ^2 behavior
- δ & $\beta \ll 1$
- δ -crossover

X-Ray Reflection: Fresnel Equations

The Fresnel equations give the correct amplitudes of reflection (and refraction) for a plane wave incident on an infinitely smooth surface. Use Maxwell's equations, keeping the components of \mathbf{E} and \mathbf{H} which are parallel to the interface continuous across the interface, and keeping the perpendicular components of \mathbf{D} and \mathbf{B} continuous across the interface.

Obviously, we need to keep the polarization in mind in applying the boundary conditions. It suffices to consider the electric field as oscillating either in the plane of incidence, or perpendicular to it.

For an incident wave of unit electric field amplitude and incident at grazing angle θ , the reflected wave will have the amplitude

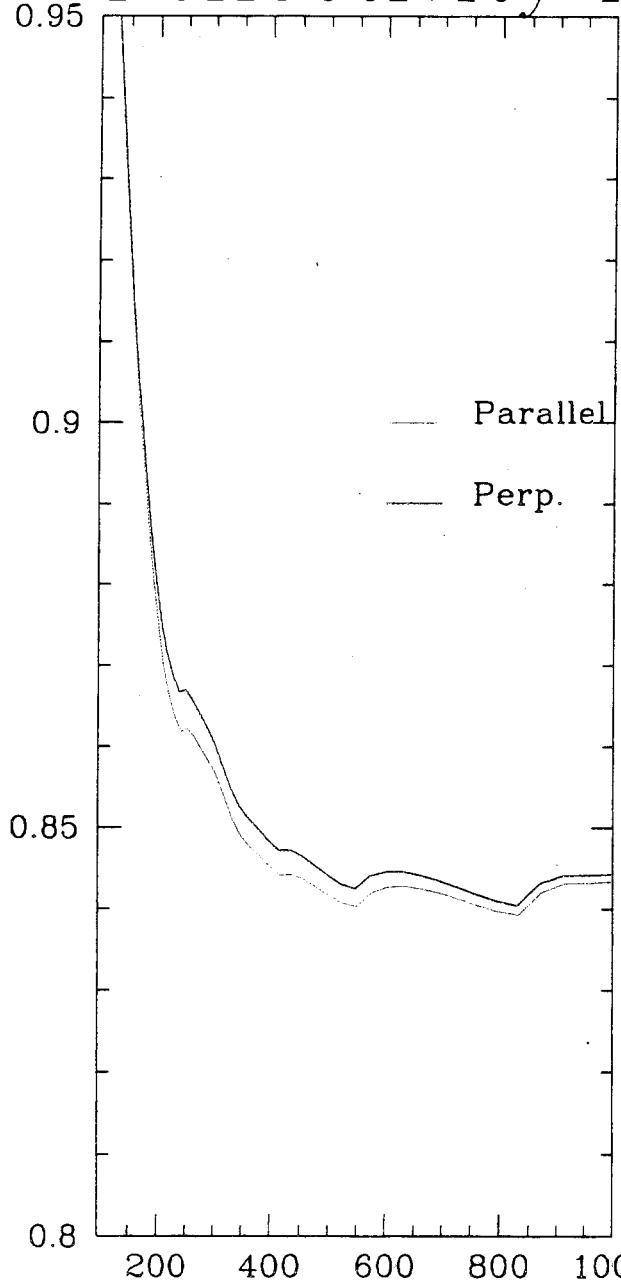
$$r_p = (n^2 \sin \theta - (n^2 - \cos^2 \theta)^{1/2}) / (n^2 \sin \theta + (n^2 - \cos^2 \theta)^{1/2}), \text{ or}$$

$$r_s = (\sin \theta - (n^2 - \cos^2 \theta)^{1/2}) / (\sin \theta + (n^2 - \cos^2 \theta)^{1/2})$$

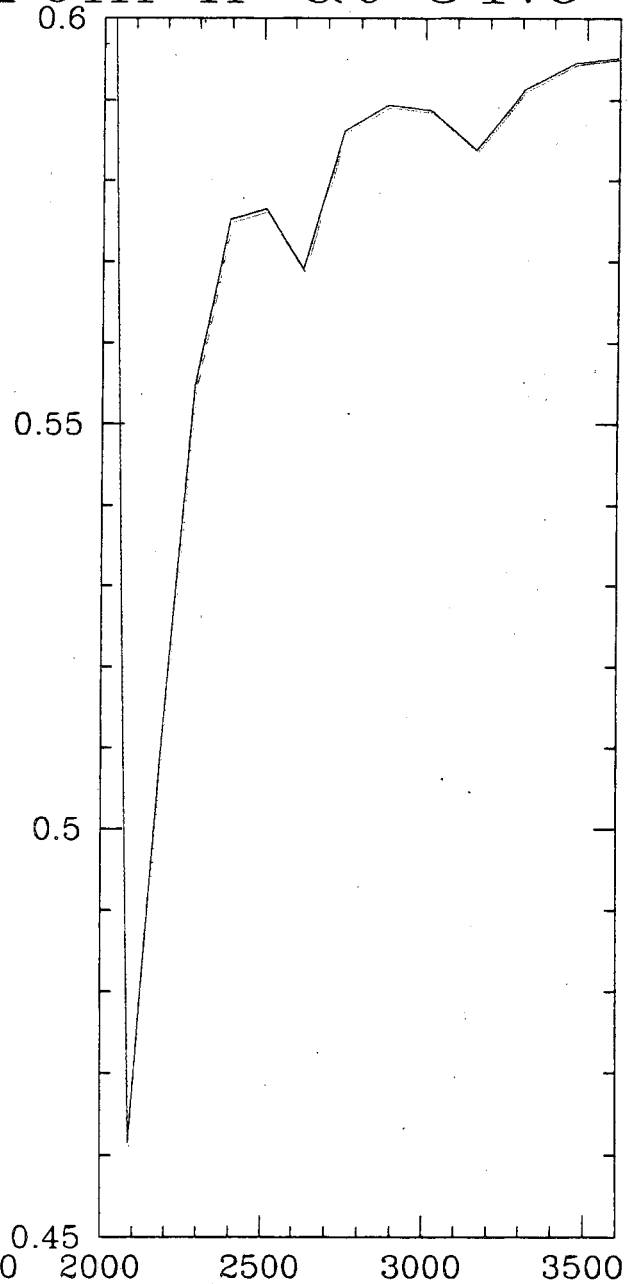
for the parallel or perpendicular components, respectively. Note that the index of refraction, n , is complex, and that the squared amplitudes of the complex numbers r_p and r_s are the actual reflectivities. For unpolarized X-rays the reflectivity is just $(|r_p|^2 + |r_s|^2)/2$

Reflectivity from Ir at 51.6'

Reflectivity



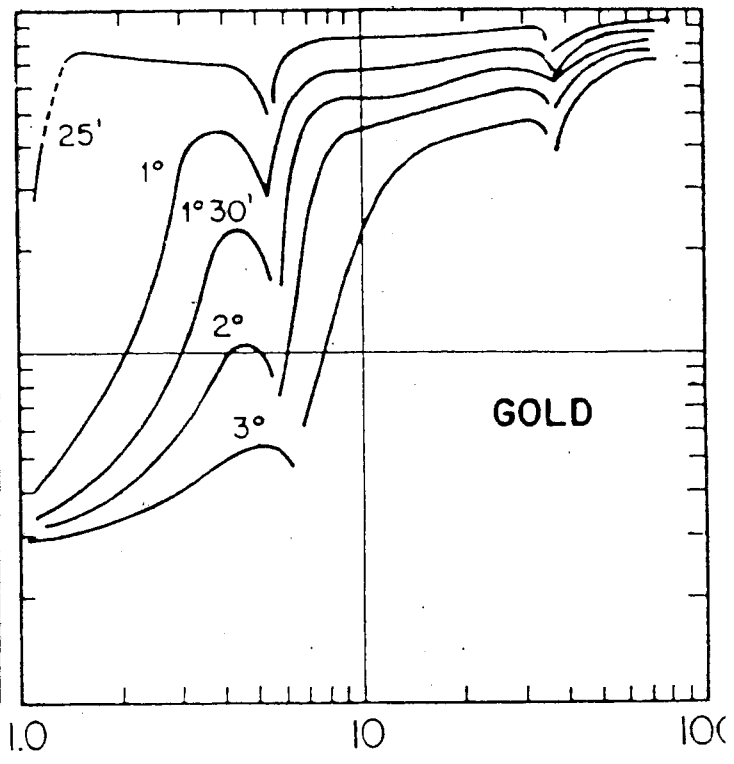
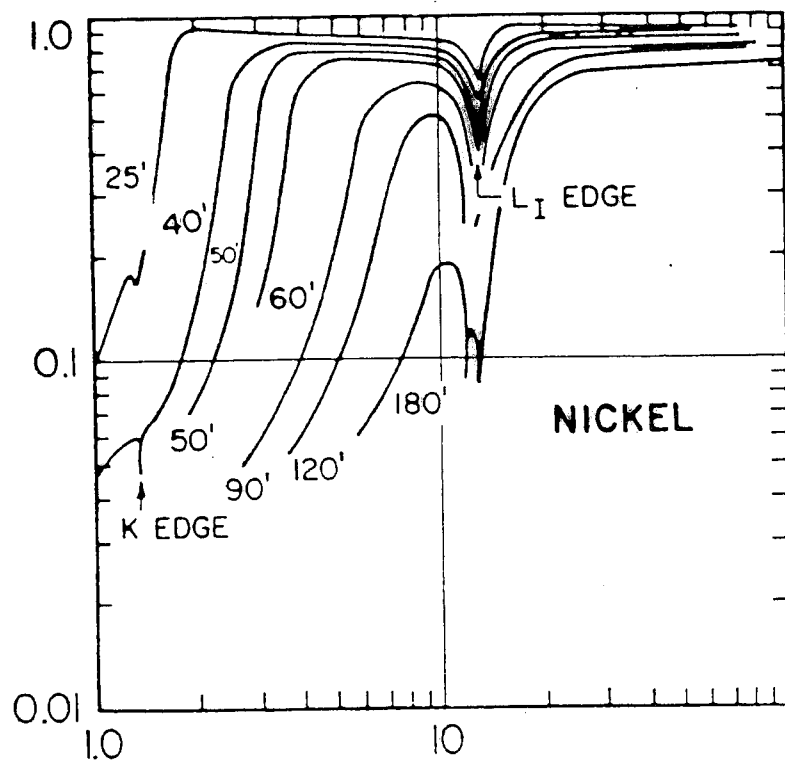
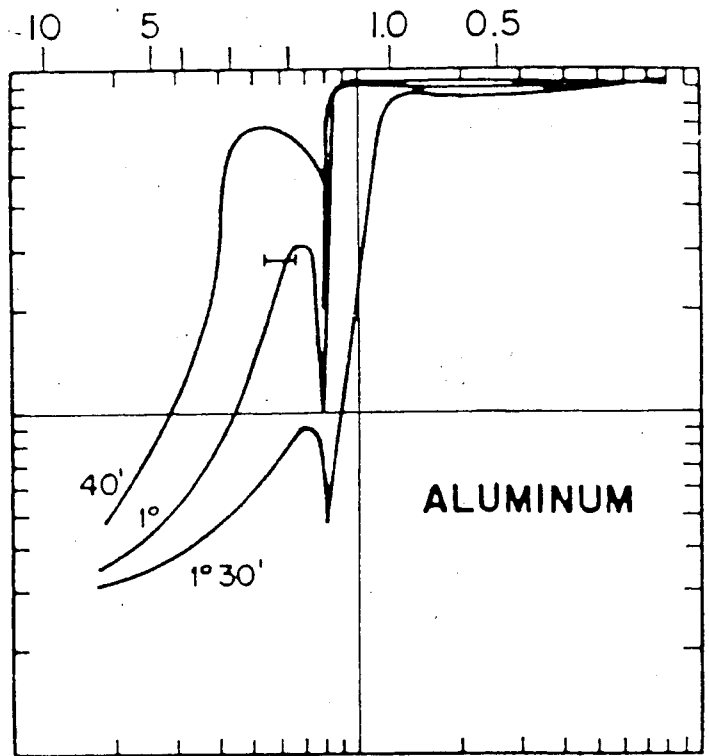
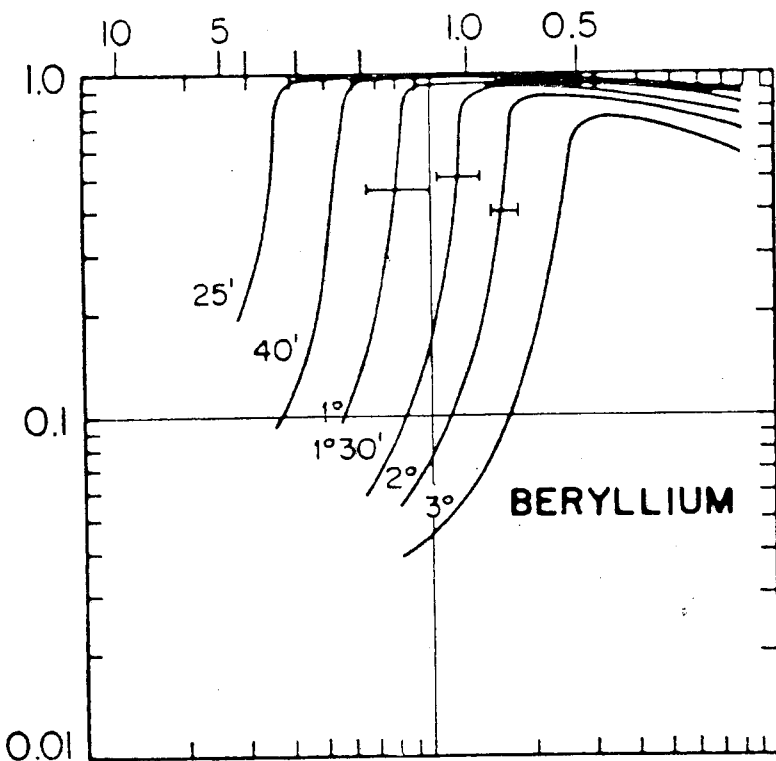
Energy [keV]



Energy [keV]

ENERGY (keV)

REFLECTION EFFICIENCY



Å

X-Ray Reflection: NOT the end of the Story

Two Significant effects remain:

1. The surfaces are not infinitely smooth. This gives rise to the complex subject of X-ray scattering. Scattering cannot be treated *exactly*, one must consider a statistical description of the surface roughness.

Key Features: Scattering increases as E^2

In plane scattering dominates by factor $1/\sin \theta$

2. We generally do not have a perfect interface from a vacuum to an infinitely thick reflecting layer. There may be
 - The mirror substrate material, e.g. Zerodur for Chandra
 - A thin binding layer, e.g. Chromium, to hold the heavy metallic coating to the glass
 - The high Z metal coating; often Au, Ir was used for the Chandra mirrors
 - An unwanted but inadvertent overcoat of molecular contaminants

Feature: Interference can cause oscillations in reflectivity.

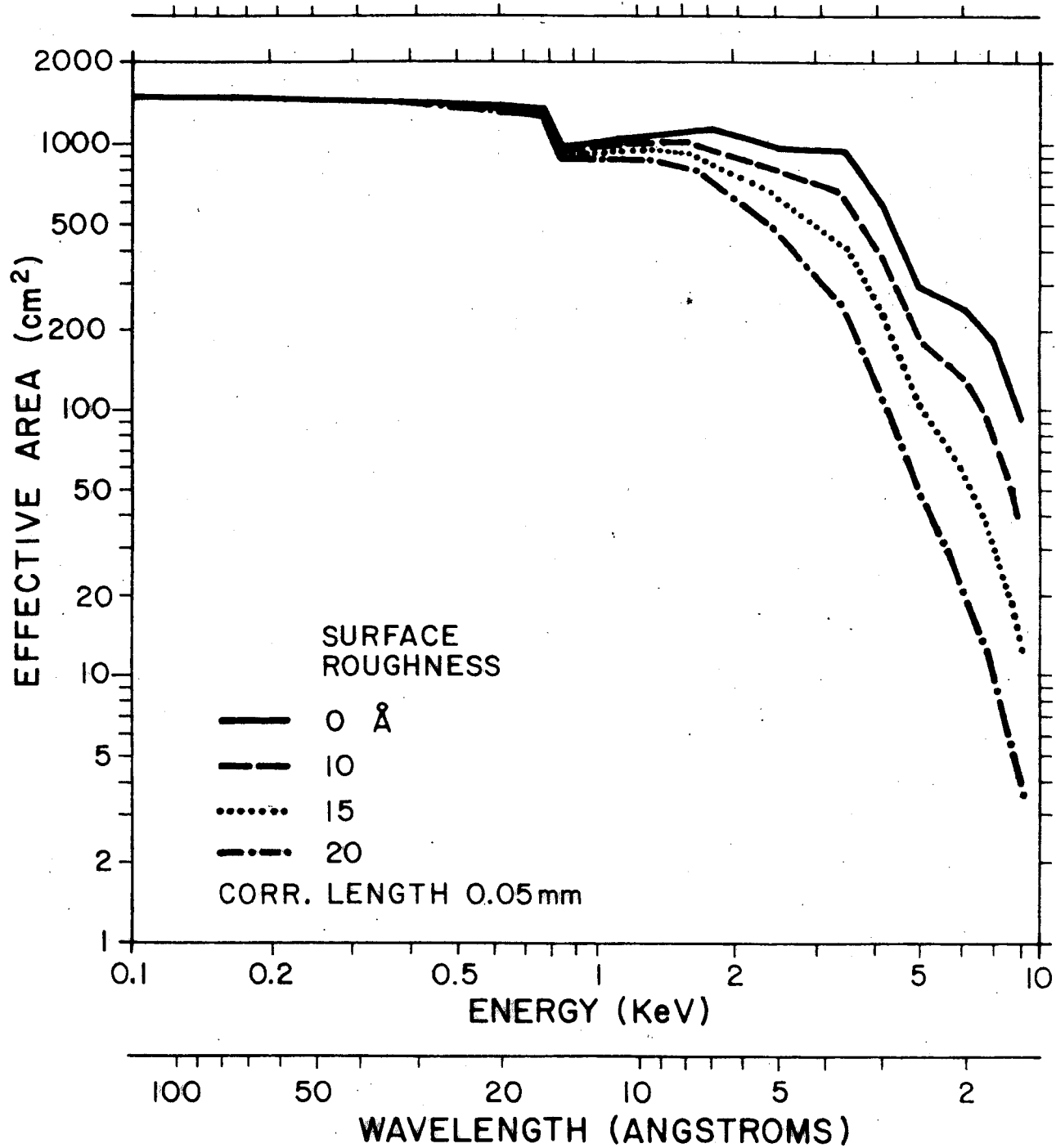
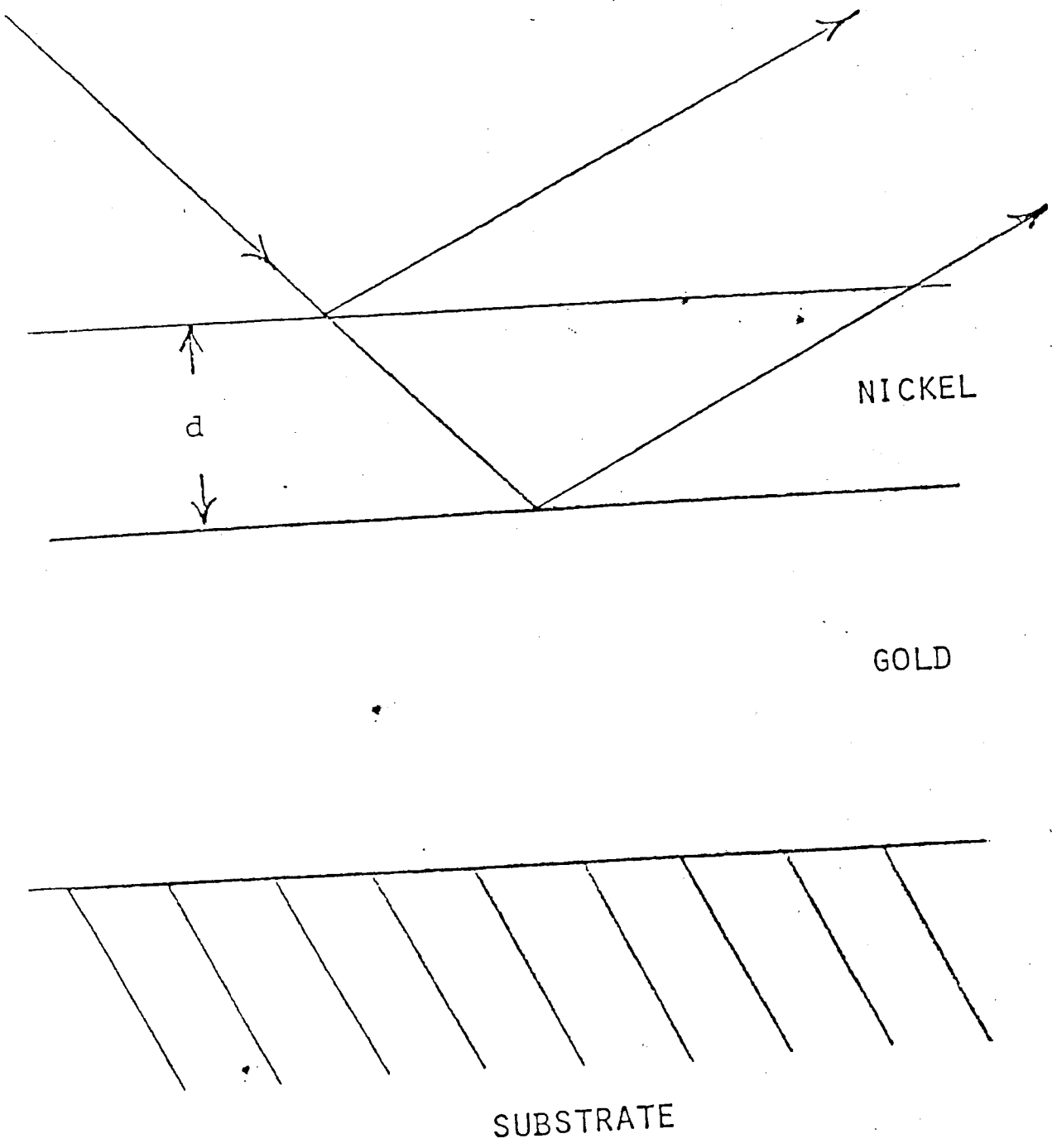


Figure 10a



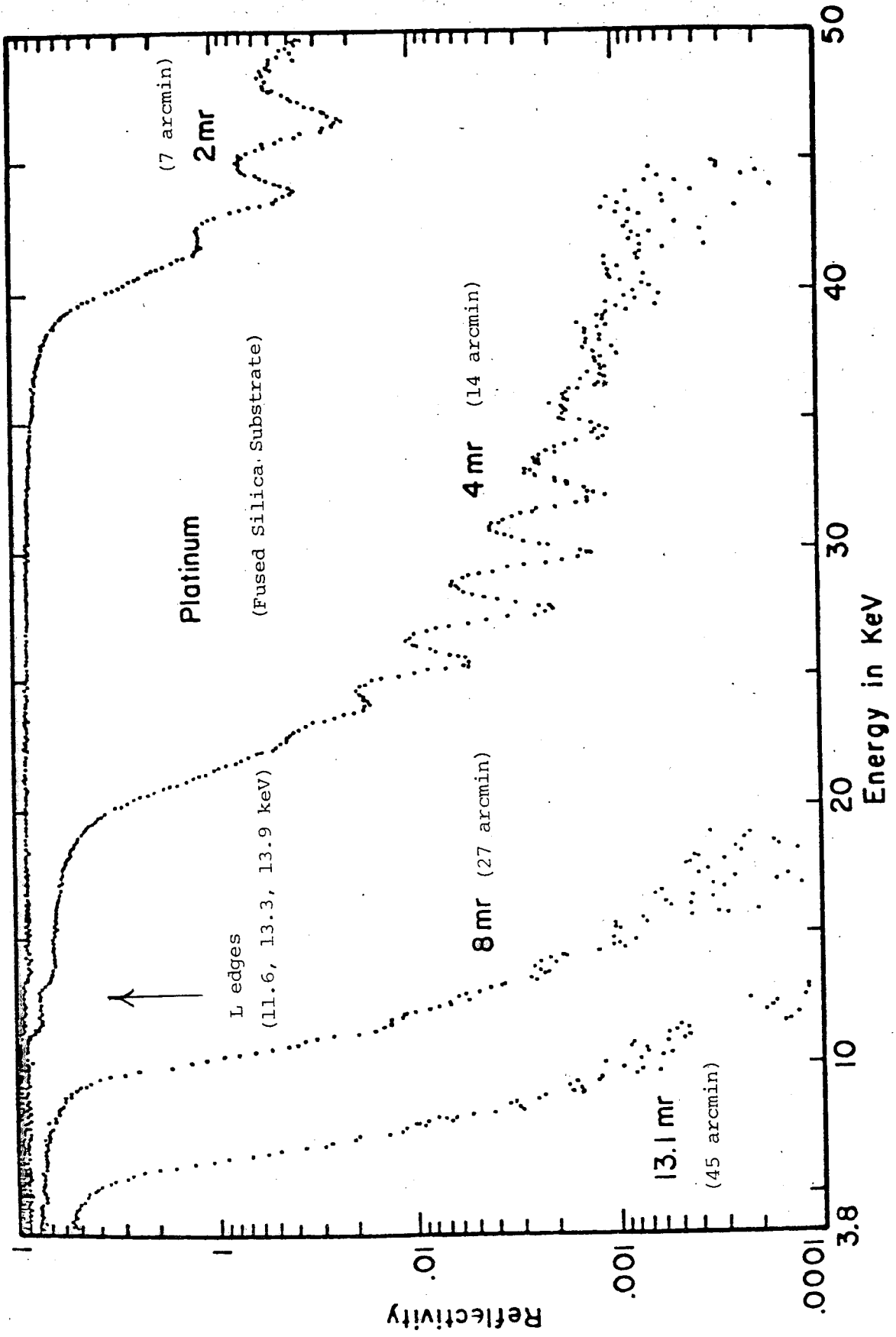
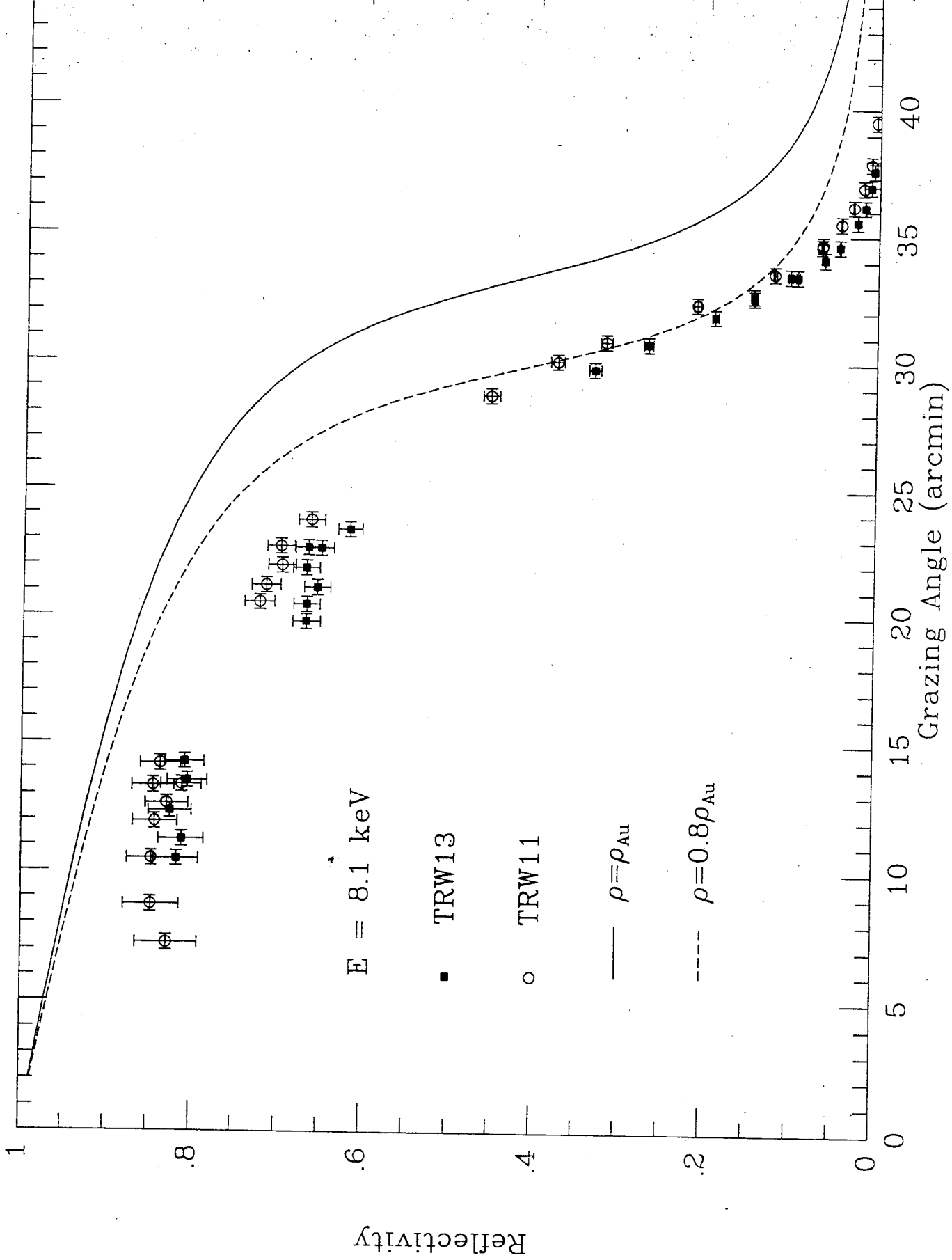


Figure 3.2 The reflectivity of a platinum coated mirror as a function of energy and grazing angle.



X-Ray Mirrors: Parabola

A parabola focusses rays which are incident parallel to its axis, to a point. If we take z along the axis, and r the distance from the axis to the parabola, an incoming ray will hit the parabola at an angle $\theta = \arctan\left(\frac{dr}{dz}\right)$ and be diverted through an angle 2θ . One verifies that $r^2 = 4fz$ satisfies the differential equation $\tan 2\theta = r/(z-f)$, where f is the distance from the origin to the focus, and can be set, e.g., by choosing that the mirror segment, of length ℓ , have a specific grazing angle α at a radius R .

We can now write some fundamental relations:

Focal Length: $F = R/2\alpha$

Paraboloid Area: $2\pi R\alpha\ell$

Parabolic Plate Area: $\alpha\ell h$

There are two uses for the parabola:

1. Translate the parabola to form a plate, curved in one dimension. This will produce one dimensional focussing of a point to a line, while another plate at right angles can focus in the other dimension.
2. Form a Paraboloid of revolution.

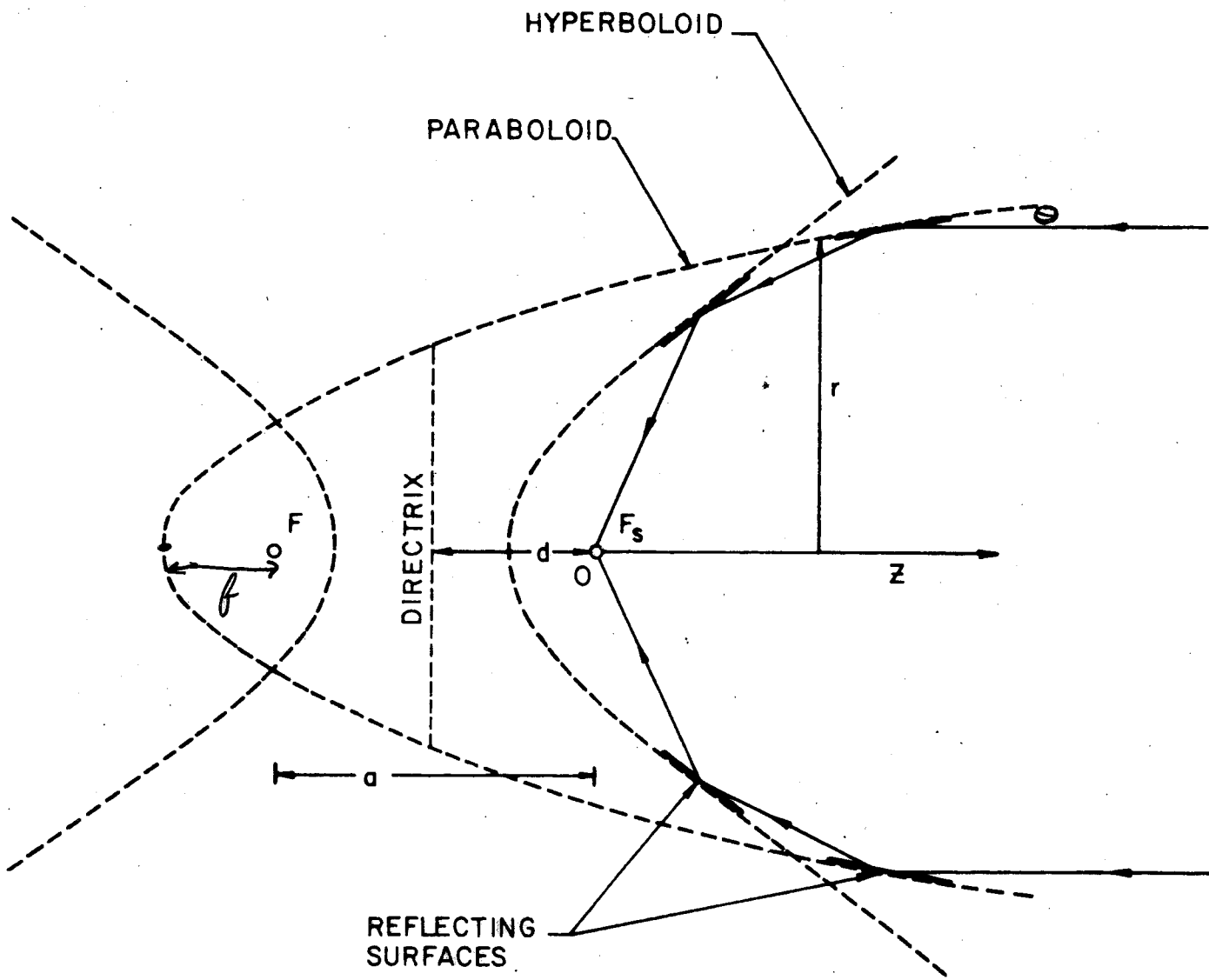
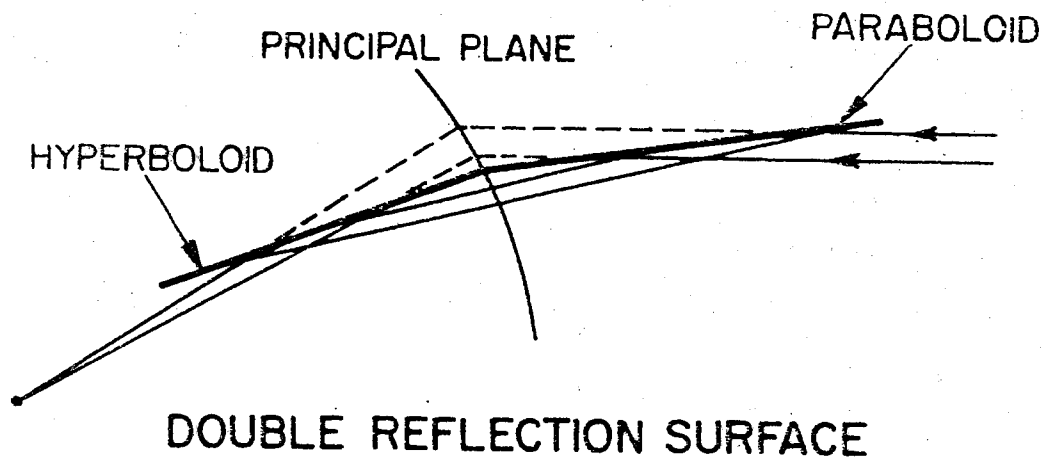
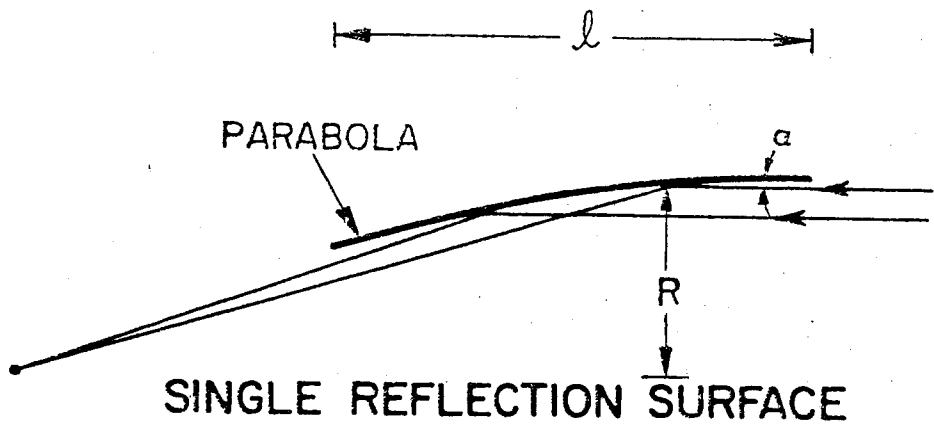
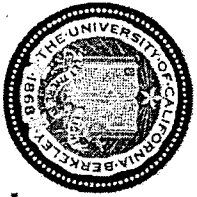


FIGURE 3 THE PRINCIPLE OF THE WOLTER TYPE I TELESCOPE. THE TELESCOPE FOCUS IS AT F_s . THE FOCUS OF THE PARABOLOID IS AT THE SECOND FOCUS OF THE HYPERBOLOID.

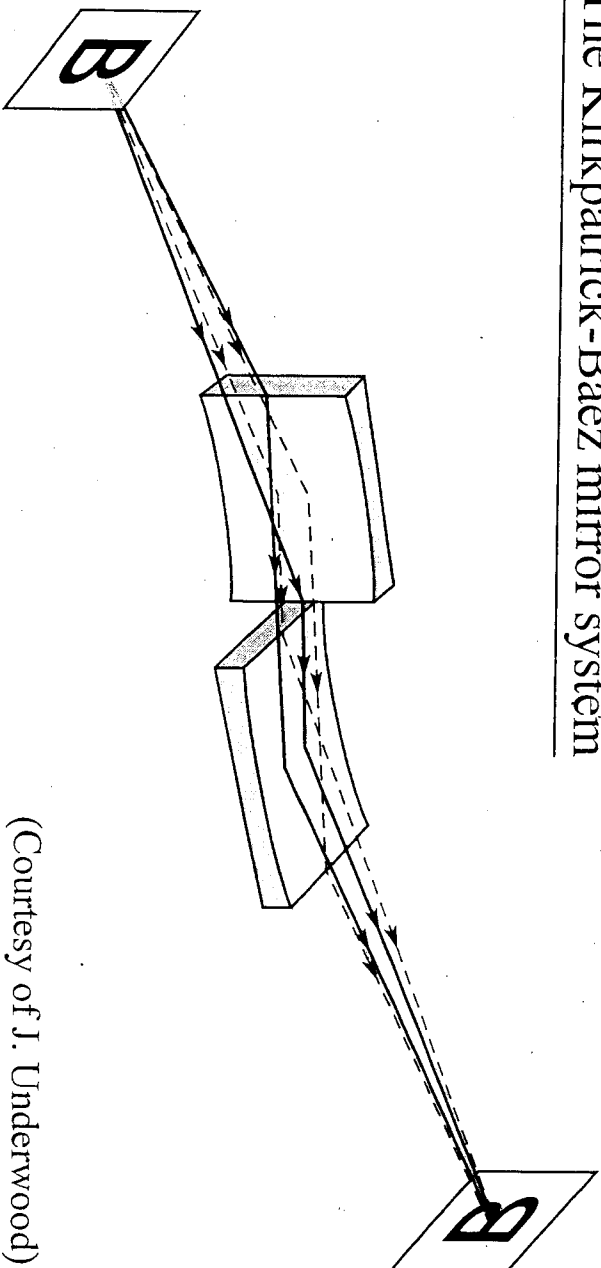


$\sigma \propto \theta^2$



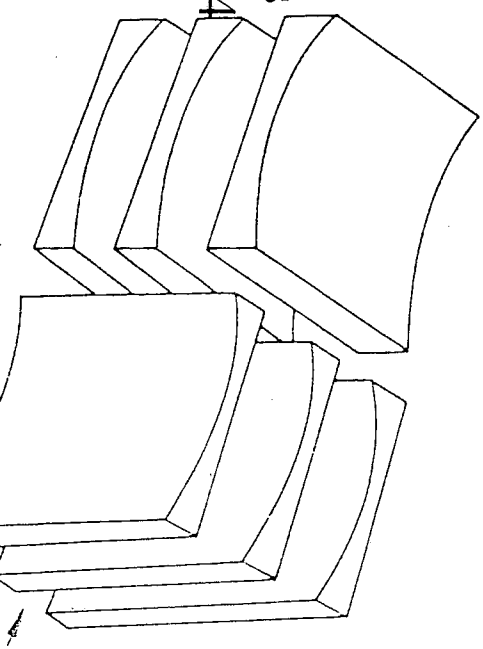
Focusing with Curved, Glancing Incidence Optics

The Kirkpatrick-Baez mirror system



(Courtesy of J. Underwood)

- Two crossed cylinders (or spheres)
- Astigmatism cancels
- Fusion diagnostics
- Common use in synchrotron radiation beamlines
- See hard x-ray microprobe, chapter 4, figure 4.14



X-Ray Mirrors: Wolter's Configurations

Wolter, H. 1952, *Ann. Physik* **10**, 94; *ibid.* 286; Giacconi, R. & Rossi, B. 1960, *J. Geophys. Res.* **65**, 773

A Paraboloid produces a perfect focus for on-axis rays. However, off-axis it gives a coma blur of equivalent image size proportional to the distance off-axis. Wolter's classic paper proved two reflections were needed, and considered configurations of conics to eliminate coma.

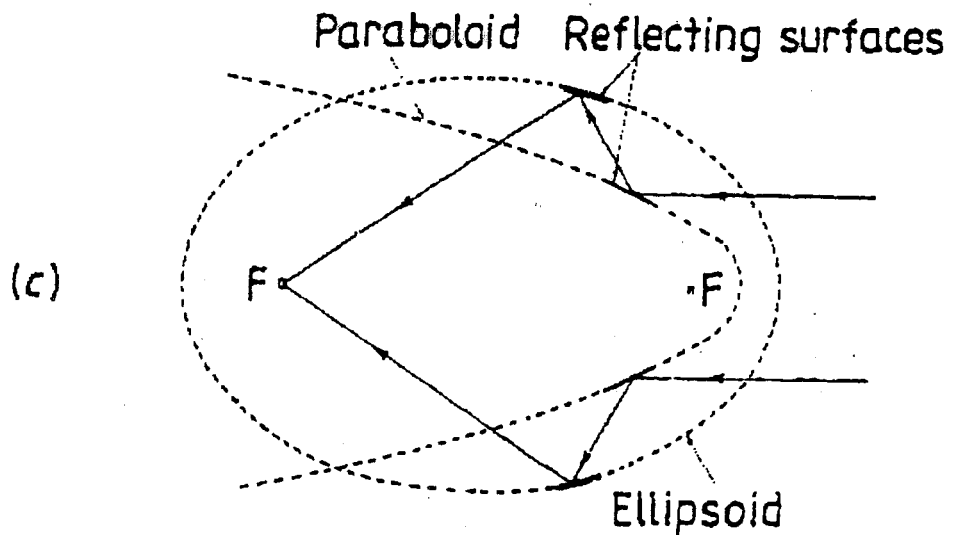
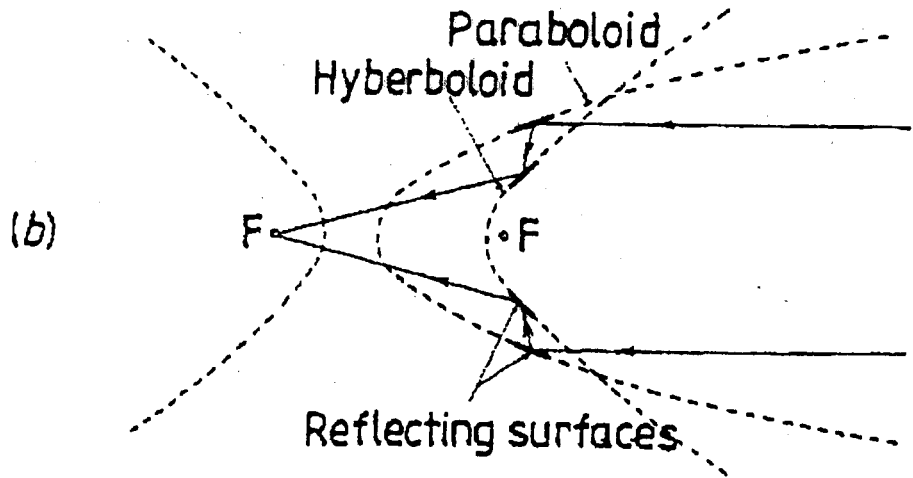
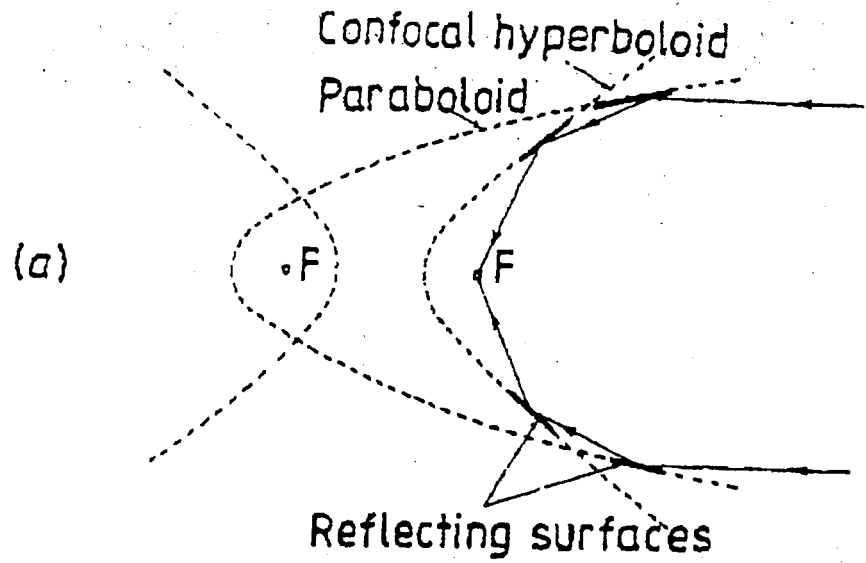
Basic Principle: The optical path to the image must be identical for all rays incident on the telescope, in order to achieve perfect imaging.

Wolter derived three possible Geometries. Of these, the Paraboloid-Hyperboloid is overwhelming most useful in cosmic X-ray astronomy:

- Shortest Focal length to aperture ratio. This has been a key discriminant as we are always trying to maximize the collecting area to detect weak fluxes, but with relatively severe restrictions on length (and diameter) imposed by available space vehicles.
- For resolved sources, the shorter focal length concentrates a given spatial element of surface brightness onto a smaller detector area, hence gives a better signal to noise ratio against the non-X-ray detector background.
- Structural advantage of the intersecting P and H surfaces. Includes mounting, nesting, and vignetting considerations. For replicated mirrors, the P and H figures are typically polished on a single mandrel and the pair formed as a single piece.

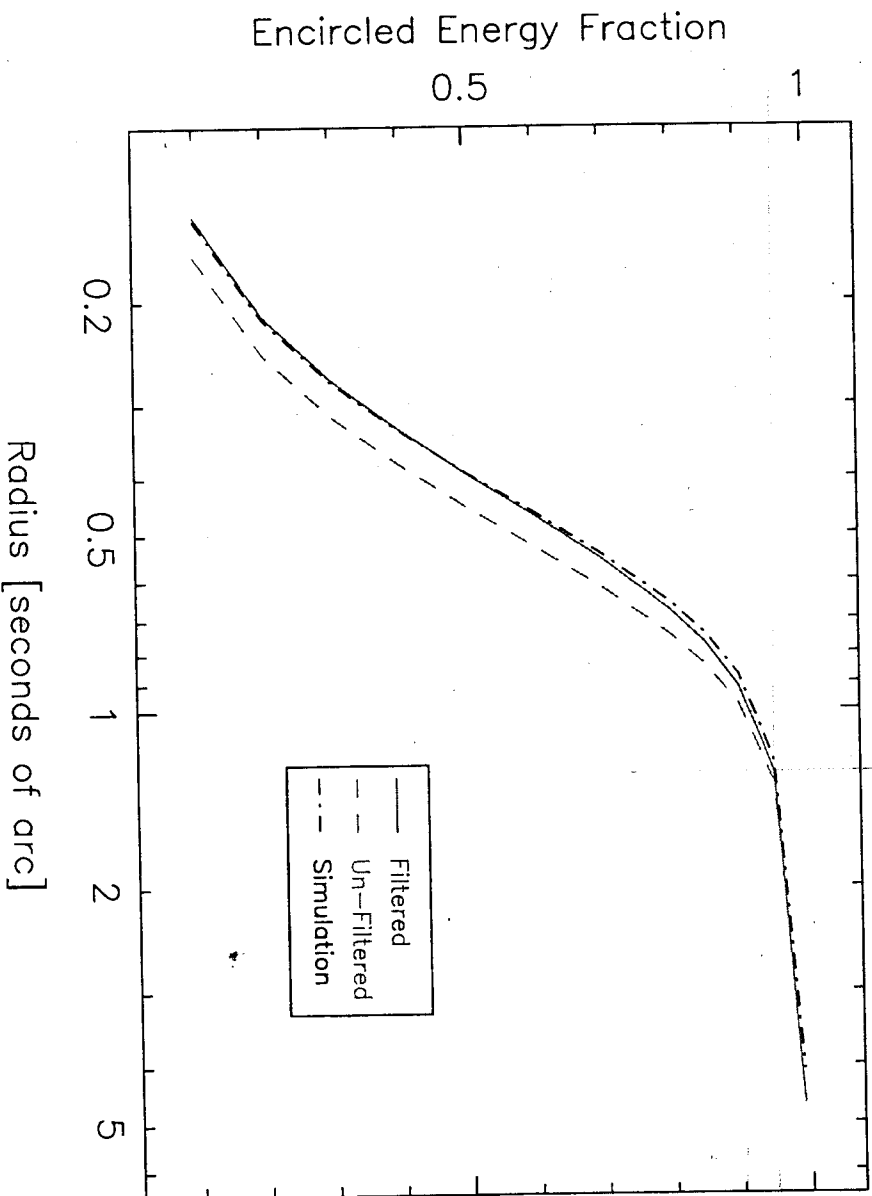
One drawback of the shorter focal length is that it puts more demand on having a detector with smaller spatial resolution in order to sample the image.

B Aschenbach



Encircled energy results, relative to flux in a 10'' radius aperture:

AR Lac [OBSID 1385]



X-ray Focus

A Grazing Incidence telescope acts as a thin lens. As the telescope tilts about small angles, the image of a point source near the axis remains invariant in space.

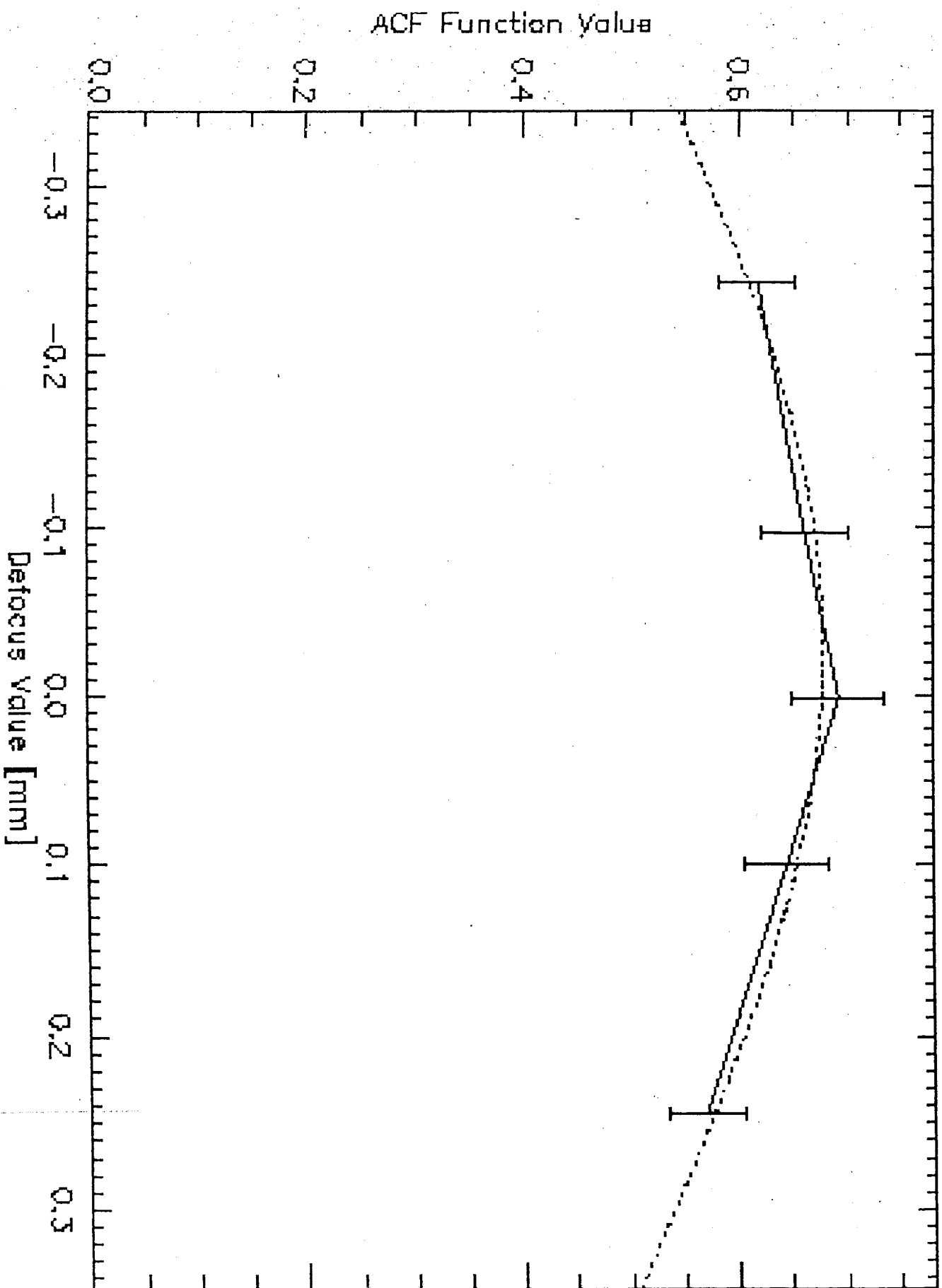
- This is what allows us to convert a linear distance y between two images to an angular distance $\theta = y/F$.
- This shows that the optimum focal surface is a bowl shape, sitting on the flat plane perpendicular to the optical axis.

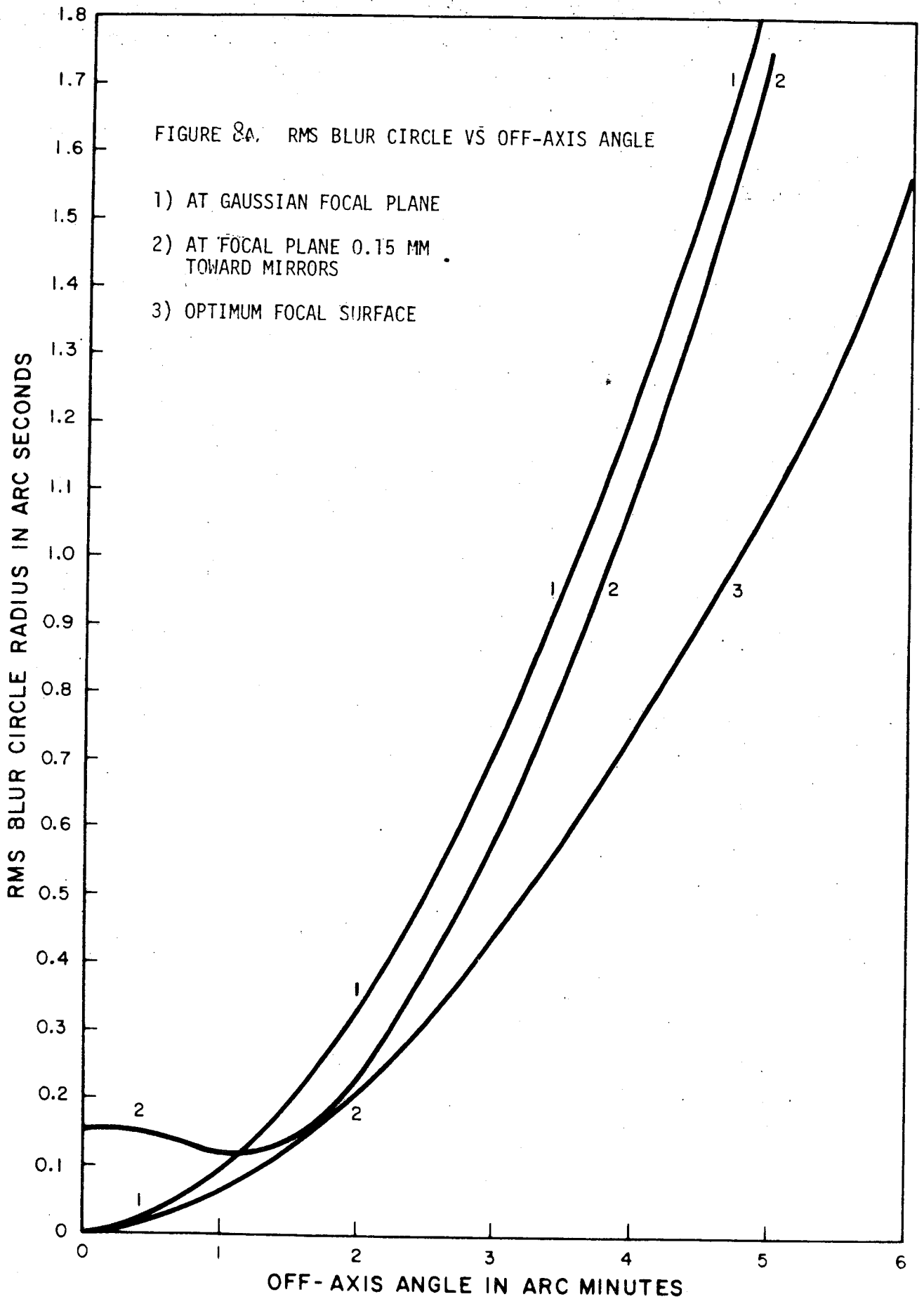
In a Wolter I system the rays from an on-axis point source converge to focus in a cone of half-angle four times the grazing angle.

For *Chandra* these cone angles are $3^\circ.417$, $2^\circ.751$, $2^\circ.429$, and $1^\circ.805$. If we budget an $0'.1$ contribution to the on-axis blur due to imprecision of the focus, then we must be able to focus within $5 \mu\text{m}/\tan 3^\circ.4 = 85 \mu\text{m}$.

Because the optimal focal plane is curved toward the mirror, and because optical imperfections in mirror figure and mechanical tolerances in aligning the pieces of glass prevent perfect imaging on axis, it is generally advantageous to position a flat imaging detector slightly forward of the ideal on-axis focus.

PG1634+706_Mar31





SPECIAL TOPIC: Multilayer Reflection

Underwood, J.2001, X-ray data booklet, sect. 4.1 (<http://xdb.lbl.gov>)

Near normal incidence reflection of soft X-rays might be of order 10^{-4} . This is because the X-rays basically penetrate the material until they are absorbed. However, even 10^{-4} reflectivity means a reflected amplitude of 10^{-2} , so if we can get ~ 100 layers to add coherently we can achieve significant reflection probability.

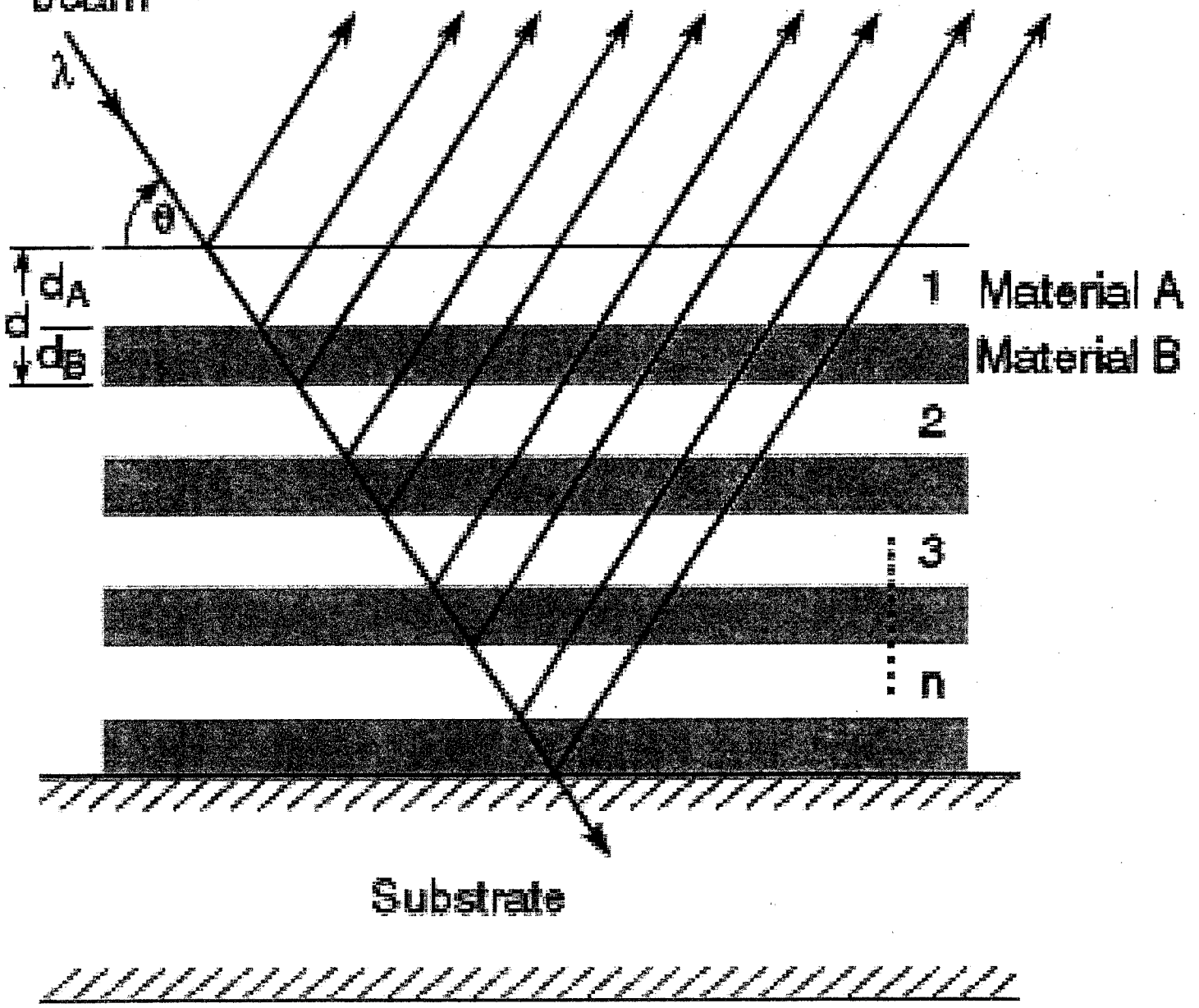
This has been realized with alternate layers of high Z material, to provide a high electron density for reflection, and low Z material, to provide a phase shift with minimal absorption.

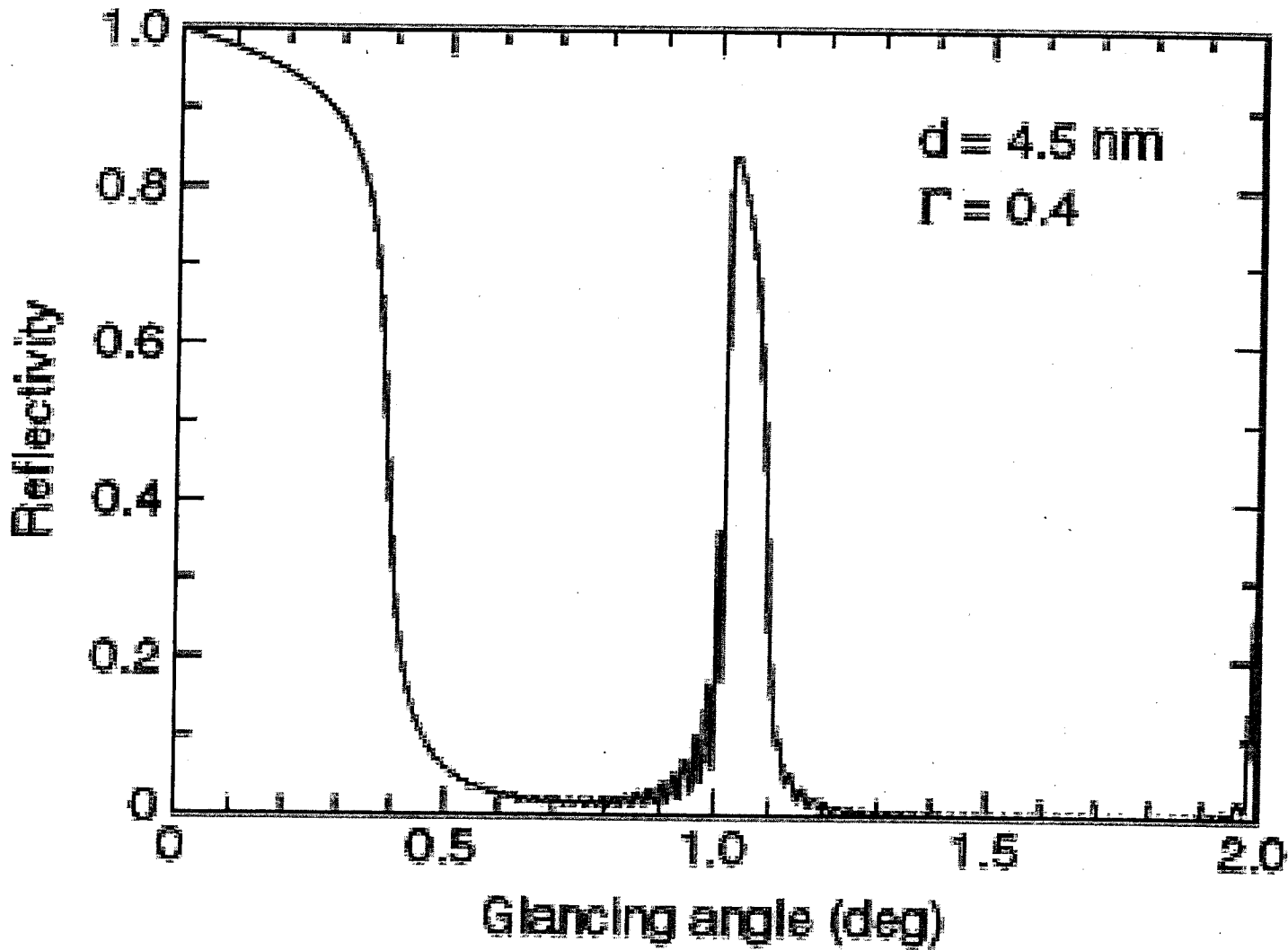
A bonus *and* disadvantage is that the resulting mirror typically only has an energy bandpass of 1% to 10%. For solar physics, Golub and colleagues have used normal incidence mirrors with outstanding success imaging selected pass bands.

Multilayers currently are being studied intensively for application at grazing incidence angles in the 10's of keV range.

Incident beam

Reflected beams





Scattering

Aschenbach, B. 1985, Rep. Prog. Phys. 48, 579; Zhao, P. & VanSpeybroeck, L. P. 2002, SPIE 4844.

Scattering theory treats irregularities in the surface height h as random, characterized by a power spectral density function

$$2W_1(f) = \left| \int e^{i2\pi x f} h(x) dx \right|^2$$

For sufficiently smooth surfaces scattering can be considered as diffraction, so that light of wavelength λ is scattered due to irregularities with spatial frequency f according to the usual grating equation:

$f = \epsilon \sin \alpha / \lambda$, where α is the grazing angle and ϵ the scattering angle.

The scattered intensity, relative to the total power in the focal plane,

is $\psi(\epsilon) = 2W_1(f) 8\pi (\sin \alpha)^4 / f \lambda^4$

Features:

1. Scattering is predominantly in the plane of the incident X-ray and the normal to the surface. Out of plane scattering is less by a factor $\sin \alpha$.
2. Scattering is asymmetric. Backward scattering can be no more than $-\alpha$, which would take the ray into the surface. Forward scattering is unlimited.

For a Gaussian distribution of surface heights, and no correlation of roughness with direction, the relative total scattered intensity is $1 - e^{-(4\pi\sigma \sin \alpha / \lambda)^2} \sim (4\pi\sigma \sin \alpha / \lambda)^2$ when the exponent is small. The rms roughness of the surface, σ is defined as $\sigma^2 = \int 2W_1(f) df$.

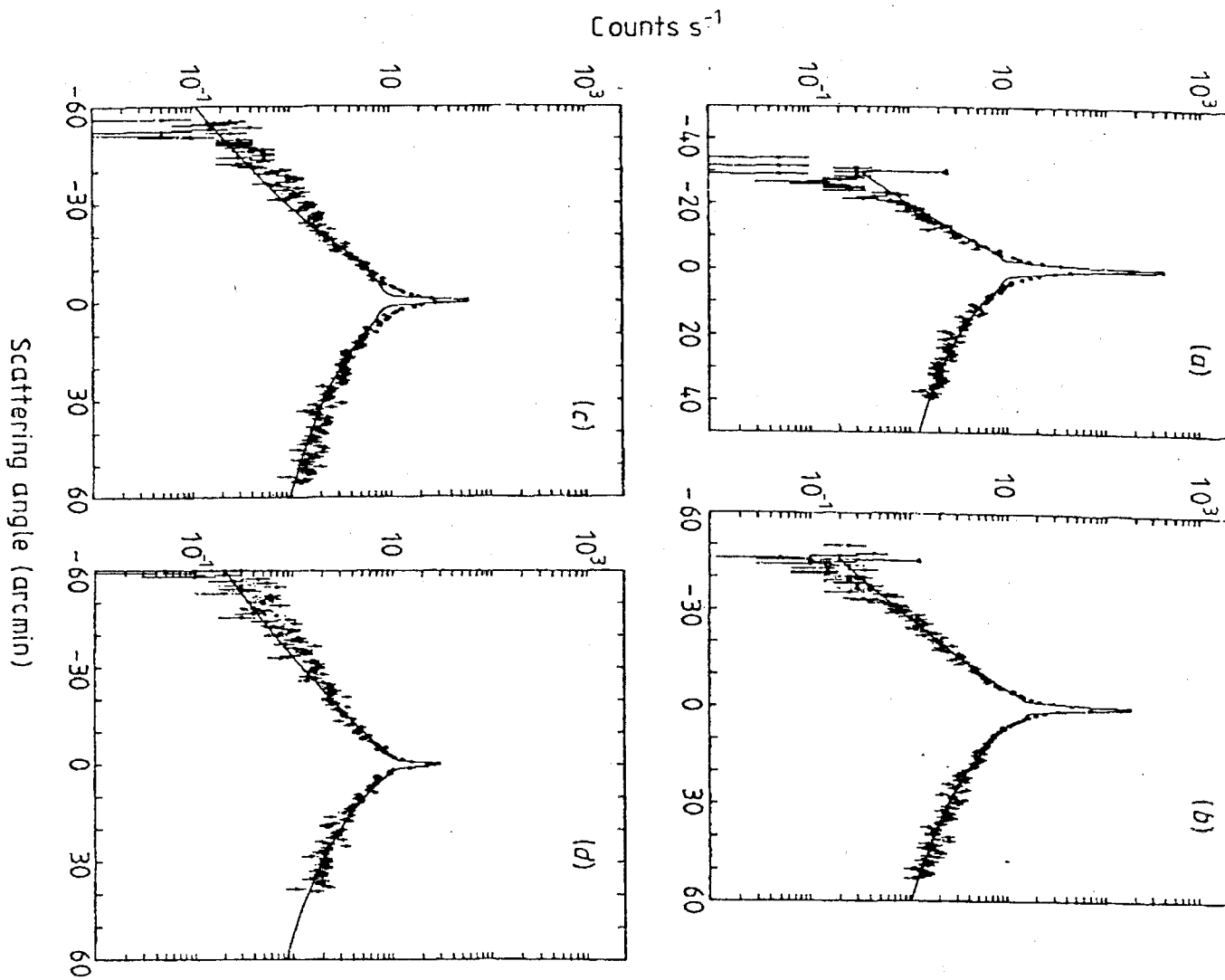


Figure 3. Comparison of measured and theoretical scattering distributions in the plane of incidence of a Kanigen flat sample at $\lambda = 13.3 \text{ \AA}$ for grazing angles $\alpha = 0.5^\circ$ (a), 0.75° (b), 1.0° (c) and 1.25° (d) (Lenzen 1978).

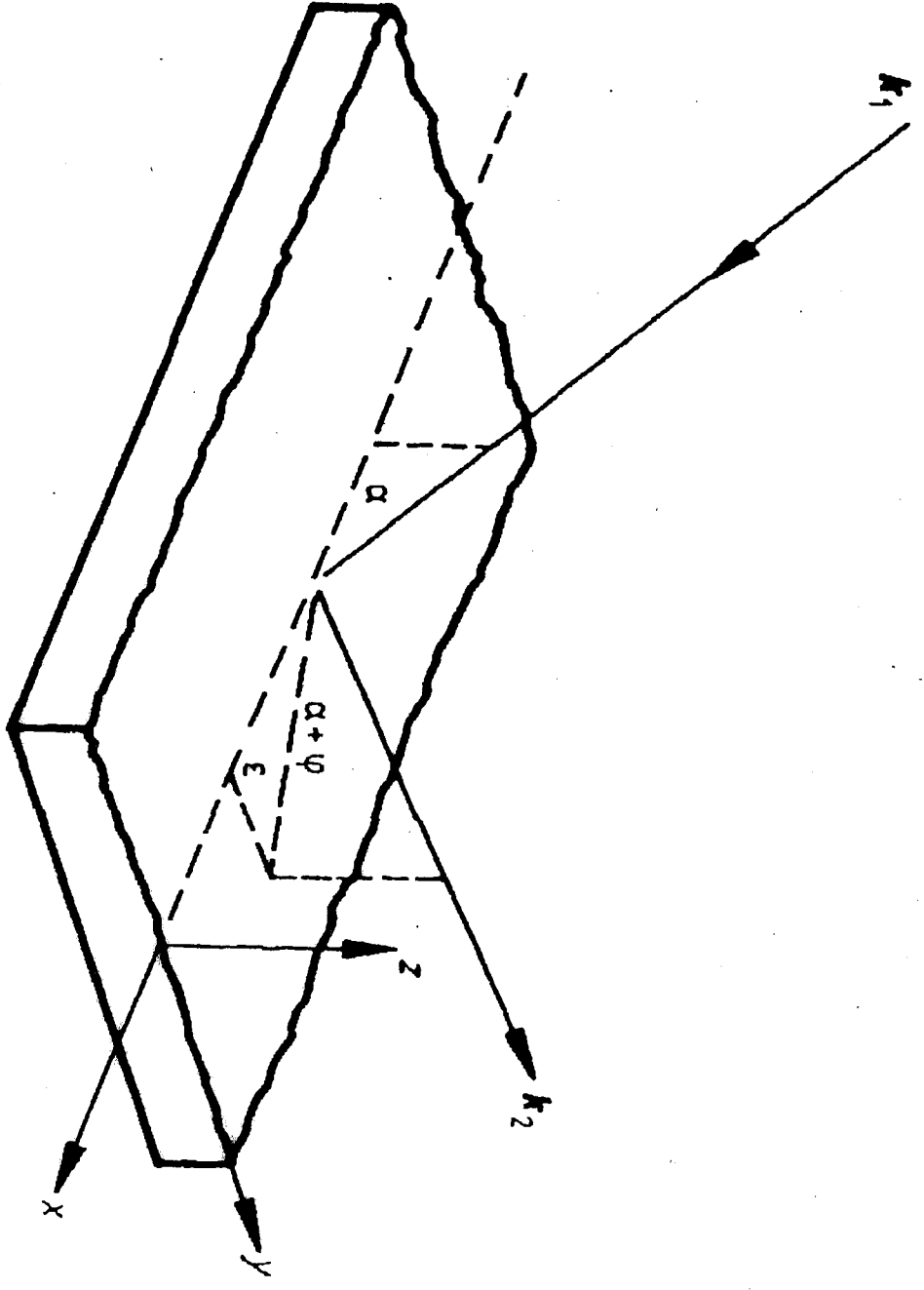


Figure 1. Scattering geometry. k_1 and k_2 denote the wavevector of the incident and scattered ray, respectively.